Cochlear Implants: bridging the gap between computational model and clinic

Kalkman, R.K.

Chapter 4

Stimulation of the Facial Nerve by Intracochlear Electrodes in Otosclerosis: A Computer Modeling Study

Johan H.M. Frijns
Randy K. Kalkman
and Jeroen J. Briaire

Otology & Neurotology 2009 (30), 1168–1174

Abstract

Hypothesis: The increased likelihood of facial nerve stimulation (FNS) with cochlear implantation in advanced cochlear otosclerosis is due to a lowering of the facial nerve excitation threshold with increasing bone demineralization. Background: Facial nerve stimulation can complicate cochlear implant fitting, often necessitating the deactivation of certain electrode contacts.

Methods: High-resolution computed tomographic scans were used to estimate anatomic features of the cochlea and the facial nerve canal. These features were added to a detailed computational model of the implanted human cochlea to examine the consequences of increased conductivity of the bone of the otic capsule. The model took into account the electrode contact type (banded or otherwise) and position (perimodiolar or lateral wall) of the electrode array.

Results: Contrary to the hypothesis, facial nerve thresholds were found to be slightly elevated with increased conductivity of the surrounding bone. However, the threshold and most comfortable loudness levels of the auditory nerve increase more rapidly owing to the reduced current density in the scala tympani as current leaks more easily out of the cochlea. Lateral wall electrodes were predicted to result in an increased likelihood of FNS. A progressively reduced probability of FNS was indicated for the full-band, half-band, and plated electrode arrays, respectively.

Conclusion: The clinical observation of increased FNS in cases of cochlear otosclerosis has been demonstrated in a computational model. Rather than decreased FN threshold, it is the increased levels for cochlear stimulation that is the main factor. Particularly, perimodiolar designs with more shielding against lateral spread of current could reduce the likelihood of FNS.

Introduction

Modern commercially distributed cochlear implants (CIs) have become widely accepted as an effective treatment of severe or profound deafness. The CI produces a sensation of hearing by delivering sequences of electrical current pulses to the cochlear (VIIIth) nerve through electrodes surgically implanted in the scala tympani of the cochlea, the stimulation pulses being modulated by the incoming acoustic signal detected by an externally worn microphone.

Many commercial CIs use silastic electrode arrays that are straight before insertion, and these tend to lie along the outer ("lateral") margins of the scala tympani after insertion. Alternatively, there are several designs of "modiolus-hugging" or "perimodiolar" electrodes (usually having a preformed curved shape), which are designed to lie along the inner ("medial") margin. This results in the stimulating electrodes being located closer to the target neural elements, thus reducing the current amplitudes required and also producing more localized stimulation fields (Balkany et al., 2002; van der Beek et al., 2005; Hughes and Abbas, 2006).

Although the electrical stimulation delivered via the CI is designed to excite the VIIIth nerve, there are situations where stimulation of other nerves has been reported. This is most often in the case with the facial nerve (VIIth; FN) and is more likely to occur when relatively high stimulation currents are required. Facial nerve stimulation (FNS) usually first becomes evident during the programming of the sound processor, where stimulus-locked eye twitches or other facial movements are visible to an observer and may be felt by the patient. Usually, this occurs on a small subset of the available electrodes, and deactivation of such electrodes can still result in a satisfactory programming of the device in most cases (Muckle and Levine, 1994).

Stimulation of the VIIth nerve is presumed to sometimes occur in this way because of its close proximity to the cochlea. In some cases, FNS has been reported from electrodes close to the insertion point (cochleostomy), where the array crosses the facial ridge at the posterior tympanotomy. More often, however, FNS originates from electrodes inserted more deeply into the cochlea, most typically around the top of the first turn, close to the geniculate and labyrinthine segments of the FN (Kelsall et al., 1997).

Previous reports on the incidence of FNS in CI users have suggested widely differing figures, from 3 (Kelsall et al., 1997) to 14.6% (Niparko et al., 1991). One possible explanation for the differences in these estimates may be heterogeneity of the patient groups studied because it seems that FNS is much more commonly observed in certain deafness etiologies, notably those involving anatomic or structural changes to the cochlea. In certain situations, the FN may be closer to some part of the electrode array (as in some cases of malformation) or there might be a reduction in the resistance to current flow reaching the FN, such as fracture or loss of normal bone structure.

One such condition is otosclerosis, which involves demineralization of the otic capsule, as well as a phase of new bone growth (sclerotic phase). The functional consequences, in hearing, are a conductive hearing loss, primarily due to ankylosis of the stapes footplate,

and, less commonly, a sensorineural hearing loss due to new sclerotic bone formation within the lumens of the cochlea (Youssef et al., 1998). “Retrofenestral” or “cochlear” otosclerosis is relatively uncommon but can cause hearing loss sufficiently severe to indicate the use of a CI. Such cases constitute a small but significant proportion of CI recipients, with 6.7% reported by Rotteveel et al. (2004) in a multicenter survey involving a total of 788 adult recipients.

The severe demineralization can cause difficulties with surgical insertion of the electrode array (Ramsden et al., 1997), and the incidence of FNS in CI users has been reported to be much higher in those with cochlear otosclerosis than in the general population; in the study of Rotteveel et al. (2004), 38% of the population with otosclerosis had experienced FNS at some point. It is generally assumed that FNS primarily occurs due to the increased conductivity of the bone insulating the scala tympani from the FN, although the type and position of the electrodes used is also relevant, that is, the laterally positioned and banded electrodes are more likely to produce FNS (Jaekel et al., 2004; Ramsden et al., 2007).

For several years, a detailed computer model of the cochlea has been developed at the Leiden University Medical Center (Frijns et al., 2000; 2001; Briaire and Frijns, 2005), which has been used to gain insight into the working mechanisms of electrical stimulation of the auditory nerve by a CI. On several occasions, the model predictions were in accordance with animal and psychophysical experiments (Frijns et al., 2000; Briaire and Frijns, 2005; Frijns et al., 2009). With this model, it is possible to predict the current flow through the cochlea in far greater detail than is possible from experimental studies. It is also possible to model current flow using different electrode types and positions. In addition, as long as the model can be validated by experimental studies, it can be used to predict the consequences of changes in either the dimensions or the conductivity values of the constituent components, such as might occur in a range of pathologic conditions.

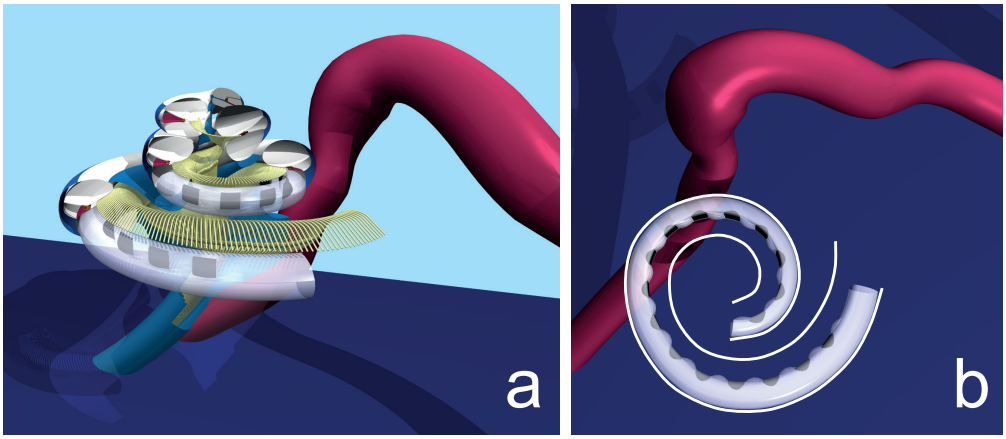

Figure 4.1. *Panel a: partly sliced-open version of the 3-dimensional model of the implanted human cochlea and the modeled segment of the FN. Panel b: the FN segment in relation to the model of the laterally inserted plate contact electrode array. The contours of the basal scala tympani are indicated by white lines.*

For the present study, we extended our computational cochlear model to include the FN in examining the effects of some of the variables relating to the production of FNS by a CI in the otosclerotic ear. A particular goal was to test the assumption that FNS is due primarily, or solely, to an increase in the conductivity of the bone surrounding the cochlea. Further goals were to examine the impact of whether the electrode array was in a lateral or perimodiolar position within the scala. Finally, it was questioned whether the nature of the electrode contact design could be demonstrated to influence the likelihood of FNS, as has been reported from clinical observations (Jaekel et al., 2004; Ramsden et al., 2007).

Materials and methods

This study used the CI model presented in previous publications from the Leiden University Medical Center, which consisted of a volume conduction model and a neural model of the auditory nerve fibers (Briaire and Frijns, 2000; Frijns et al., 2000; Frijns et al., 2001; Briaire and Frijns, 2005; Frijns et al., 2009). The volume conduction model was based on the boundary element method, and its geometry was a realistic representation of the implanted human cochlea, describing the boundaries between different media in the cochlea with quadratically curved triangles. Each medium in the model is considered purely resistive, having its own specific electrical conductivity that is the same in all directions (isotropic), and has no capacitative properties. The neural model was based on the nonlinear generalized Schwarz and Eikhof-Frijns model of primary auditory nerve fibers and used a nerve fiber morphology designed to accurately represent the human auditory nerve (Briaire and Frijns, 2005).

Compared with the previous publications, a number of changes were made to the basic model to more accurately describe the anatomy of the cochlea. Data from Stakhovskaya et al. (2007) have been implemented to generate realistic oblique fiber trajectories instead of the purely radial trajectories used in previous publications. Furthermore, the axons of the nerve fibers have been bundled together in the modiolus rather than extending from their cell bodies in parallel trajectories. The auditory nerve bundle that extends from the cochlea was therefore much narrower than in previous studies, and it followed a more realistic trajectory instead of running parallel to the cochlear rotation axis. A layer of cerebrospinal fluid was added around the nerve trunk, and a cerebrospinal fluid compartment was added inside the modiolus itself. From electrical field imaging (EFI) recordings (Vanpoucke et al., 2004) in patients, a more accurate value of the conductivity of the temporal bone and the modiolus was determined for the model, giving a new bone conductivity value of 0.016 S/m and a modiolus conductivity of 0.2 S/m. With these adapted parameter values, simulated electrical field potentials are in line with actual recordings.

Three different electrode arrays were designed: 1) an equivalent of the Nucleus Straight (Cochlear Ltd., Sydney, Australia) electrode array having a banded annular contact design (with 22 contacts), 2) a version of the Nucleus Straight array model with 22 half-banded electrode contacts (more or less mimicking the Contour array), and 3) an equivalent of the Advanced Bionics HiFocus (Sylmar, CA, USA) electrode array having 16 flat modiolar-facing

plate contacts. The electrode contacts were labeled from 1, for the most basal to 16 of 22 for the most apical contact.

For this study, the dimensions of the FN canal and its orientation relative to the cochlea were ascertained from high-resolution computed tomographic (CT) scans of a patient with otosclerosis (Verbist et al., 2005; 2008) to derive a new model of the FN. The dimensions and shape of the cochlea model were adjusted to match those of the CT scan, giving us a combined cochlea/FN model, which included a segment of the FN as illustrated in Figure 4.1a. The CT scans of the patient with otosclerosis showed a layer of approximately 1-mm thickness around the cochlea where the bone was denser than the surrounding bone. Therefore, such a layer was added to the cochlear model.

The neural response properties of the FN were defined in a similar way to our existing model of the auditory nerve based on the nonlinear generalized Schwarz and Eikhof-Frijns model of primary auditory nerve fibers (Briaire and Frijns, 2000; Frijns et al., 2000; Briaire and Frijns, 2005). The model simulated the response to time-varying potential fields in the cochlea and was applied to both the auditory and the FNs. A bundle of 16 homogenous fibers was positioned along the outer contour of the FN canal. Dimensional characteristics of these fibers were based on data from Schröder et al. (1988), including a 4-μm axonal diameter and 400-μm internodal spacing. Each FN fiber consisted of 88 nodes of Ranvier, resulting in a 34.9-mm section of the FN in closest proximity to the contacts of the electrode array implanted into the scala tympani of the cochlea (Fig. 4.1b).

The primary measures of interest were excitation thresholds of the cochlear nerve and the FN (in mA) and the most comfortable loudness (MCL) levels of the cochlear nerve. As previously, the MCL was defined as the current required to exceed the threshold for a length of 4 mm along the basilar membrane (Frijns et al., 2009). From these measures, it was possible to predict where FNS was likely to occur relative to the auditory dynamic range; that is, whether FNS would reduce the useable dynamic range of an electrode contact or prevent its use completely. Stimulus parameters were symmetrical biphasic current pulses with a phase duration of 37.5 microseconds delivered to each individual electrode contact for the 3 electrode array models. For the purposes of modeling, each electrode array was studied in both lateral and perimodiolar (medial) positions. Note also that to ensure calculations would be made in a comparable manner for each of the electrode array designs, the banded electrode array is modeled as more deeply inserted than would normally be found in clinical practice with the Nucleus Straight array. The main effect of this would be to show the worst-case FNS occurring at different electrode contacts than might be encountered clinically. Because an exact conductivity value of otosclerotic bone is not known, we have performed the above calculations for various bone conductivity values. The lower limit of the conductivity range was 0.016 S/m thought to represent that of a typical healthy otic capsule, whereas for the upper limit, a value of 1.6 S/m was chosen, representing a considerable increase in the ability of electrical current to pass through the demineralized otosclerotic bone (for comparison, perilymph has a conductivity of 1.43 S/m). The dense bone layer around the cochlea was assumed to have a 50% lower electrical conductivity than the normal temporal bone (0.008 S/m).

Results

Figure 4.2 shows the effects of increasing bone conductivity on the excitation thresholds of the FN and cochlear nerve and on the MCL of the cochlear nerve. The situation for full-band, half-band, and plate contacts is shown in the top, middle, and bottom panels, respectively. The 3 panels on the left show results for each electrode array located at the lateral (outer) extent of the scala tympani, whereas the 3 panels on the right show the situation when the electrode array has been placed in a perimodiolar (medial) position. The stimulating electrode illustrated in Figure 4.2 was the one producing the lowest FN threshold by electrode array type: E13 for the lateral full-banded and half-banded arrays, E15 for the medial-banded arrays, and E11 for the plate arrays. In fact, all these contacts were located at an insertion angle of approximately 280 degrees from the round window.

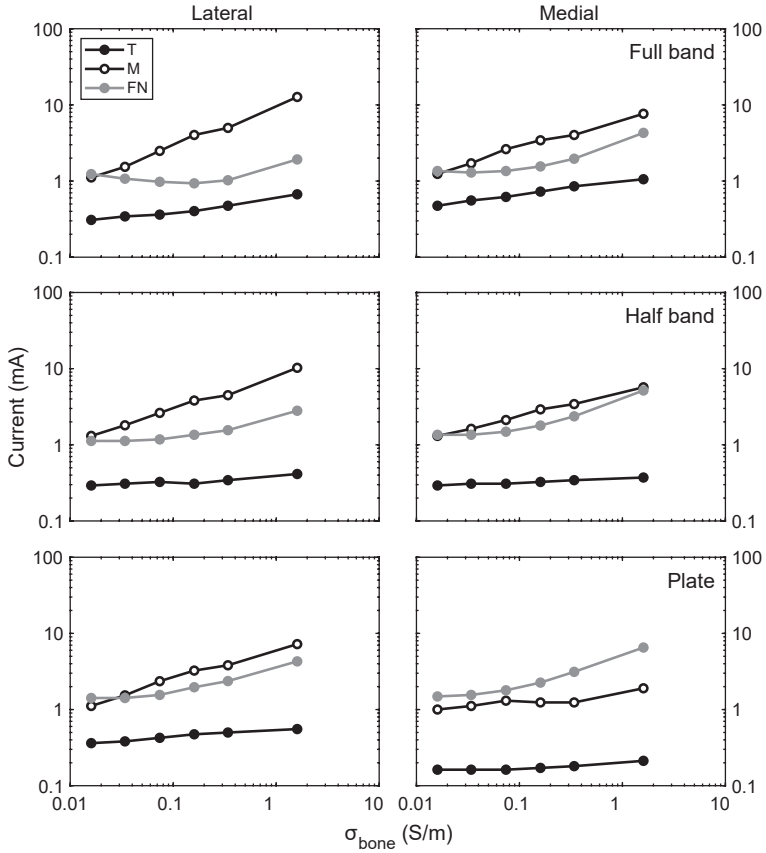

Figure 4.2. *Facial nerve thresholds (filled circles, gray line), cochlear nerve thresholds (filled circles, black line), and cochlear nerve MCLs (open circles, black line) as a function of conductivity of the surrounding bone. Plots are included for a full-banded electrode array (upper panels), a half-banded array (middle panels), and the plate electrode array (lower panels), the latter 2 with contacts facing the modiolus. The panels on the left are for the arrays in the lateral position of the scala tympani, and the panels on the right are for arrays in the medial position. The stimulating electrode contact was the one producing the lowest FN threshold in each case.*

Note that, ideally, the half-band electrode array would take up a perimodiolar position in normal implantation and that the full-band array would normally be in the lateral position.

It is clear that, in all conditions, increased bone conductivity results in slightly increased excitation thresholds of both nerves. However, the MCL of the cochlear nerve, particularly in the lateral positions, increases at a greater rate than the excitation threshold of either nerve. This has 2 effects: 1) the electrical dynamic range of the cochlear nerve appears to be considerably larger at higher bone conductivities and 2) the threshold of FNS occurs at a lower point in the auditory dynamic range at higher bone conductivities.

Figure 4.3 shows the effect of the electrode contact position for the full-band and plate electrode contact designs. Both arrays are modeled in the lateral location. Calculations were made for 3 bone conductivity values: 0.016 (upper panels), 0.16 (middle panels), and 1.6 S/m (lower panels). These conductivities cover a range from normal, moderately

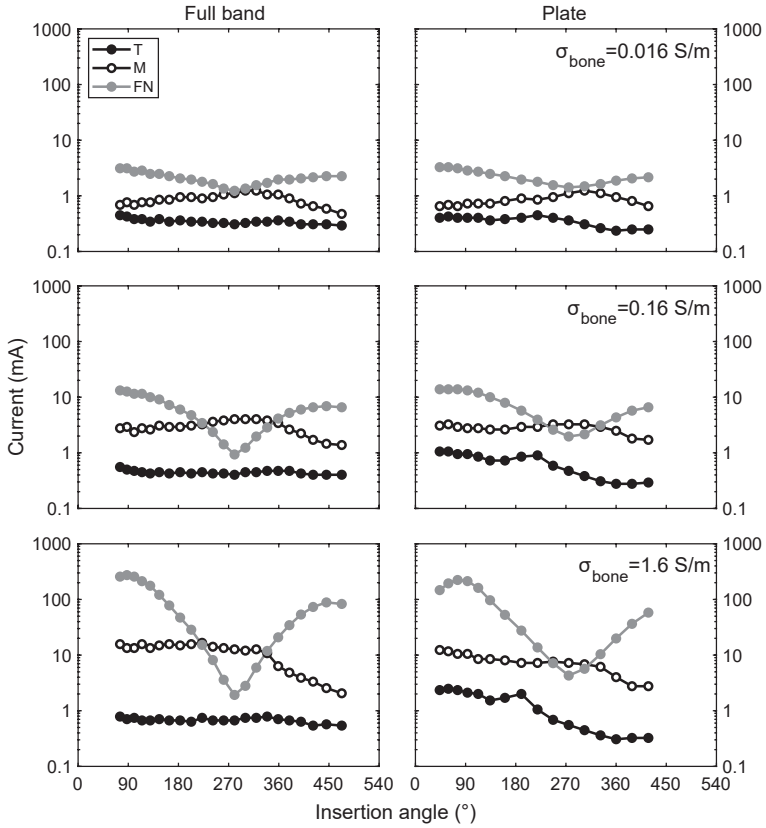

Figure 4.3. *Facial nerve thresholds (filled circles, gray line), cochlear nerve thresholds (filled circles, black line), and cochlear nerve MCLs (open circles, black line) as a function of the angular insertion depth of the stimulating electrode. Left panels are for the full-band array, and right panels are for the plate electrode array. The upper panels are results with normal bone conductivity (0.016 S/m), middle panels are results with a conductivity of 0.16 S/m, and lower panels are results with a conductivity of 1.6 S/m.*

demineralized bone to severely demineralized bone. As explained in Materials and Methods, there are no data regarding the actual conductivity value of the bone in otosclerosis.

Several observations were evident from these plots:

1. Facial nerve threshold has a minimum value at approximately the same angular position in all traces, corresponding to E13 for the full-band contact array and E6 for the plate contact array. These electrodes are in the region of the cochlea closest to the FN.
2. Facial and cochlear nerve excitation thresholds become higher with increasing bone conductivity (as is also evident in Fig. 4.2). However, FN excitation thresholds for the contacts closest to the FN are elevated less, implying an increased risk for FNS.
3. Cochlear nerve MCLs also increase with increasing bone conductivity, but more so than the thresholds, such that the auditory dynamic range also increases with increasing conductivity.
4. There are regions where FN thresholds are lower than auditory MCLs, a trend that is more evident for the electrode array with full-band contacts.
5. For electrodes toward both ends of the array, moving away from the FN location, the FN excitation thresholds are dramatically increased with increasing bone conductivity, such that they become very much higher than the auditory MCLs.

Discussion

The hypothesis that excitation of the FN by a CI is more frequently encountered in cases of cochlear otosclerosis, owing to the increased conductivity of the bone surrounding the cochlea, seems to be supported by our modeling work. However, the mechanism through which this is predicted to occur is not so intuitive. A lowering of the FN excitation threshold with increasing bone conductivity was expected. Unexpectedly, the FN excitation threshold was found to remain relatively constant for conductivities up to approximately 0.3 S/m. The main effect seemed to be an increased current being required to produce MCL with higher bone conductivity. This effect is explained by a higher leakage of stimulation current from the scala tympani as developed and discussed in later paragraphs.

In an earlier study, we examined the field patterns generated by current sources in a 3-dimensional model of the electrically stimulated cochlea (Briaire and Frijns, 2000). From this, it was evident that the highly resistive organ of Corti and the basilar membrane virtually block the current flow out of the scala tympani superiorly. The bone layer between the turns also works to confine the current flow to the scala tympani. On the other hand, the spiral ligament has much higher conductivity and appears to act as a pathway through which current can leak out of the scala tympani. In the normal ear, this is, of course, surrounded by the bone of the otic capsule, which presumably serves to isolate the FN from electrical fields originating in the scala tympani despite their proximity to the top

of the first turn. It was hypothesized that an increased conductivity of the bone could potentially reduce the threshold of the FN to stimulation by such fields.

Counterintuitively, the results of the present study show that increasing bone conductivity tends to increase excitation thresholds for both the cochlear nerve and FN, presumably owing to the reduced current density produced in the scala tympani. For FN thresholds, this effect seems much more pronounced when the stimulating contact is further away from the FN. In addition, MCLs seem to increase more than the auditory nerve thresholds (resulting in an increased electrical dynamic range with higher bone conductivities). Taken together, these factors can result in the presence of a region of the cochlea where the FN excitation threshold is lower than the MCL. This is, of course, exactly what is observed clinically in some patients, where it is not possible to reach the MCL without initiating FNS, such that these electrodes have to be deactivated in a sound processor program. Rotteveel et al. (2004) reported this effect to occur at insertion angles comparable to those predicted by the model.

The effect of raised auditory nerve threshold and MCL in implanted otosclerosis patients has been reported in association with some clinical studies (Quaranta et al., 2005; Sainz et al., 2007), although most studies do not report stimulation levels that differ from patients without otosclerosis. We also checked our own patient data and found that average threshold and MCL levels of our group of patient with otosclerosis (n = 11) were higher than those in a group of 90 patients without otosclerosis (all with a HiFocus electrode), but because of the large variability of stimulation levels in patients, no statistical significance was found. This could mean that it will be difficult to conclusively prove or falsify the model-predicted raised stimulation levels due to otosclerosis in clinical studies.

In the model, certain effects of electrode type and placement were also evident. Although the abovementioned observations were visible in all conditions tested, they were more pronounced in some conditions than in others. In Figure 4.3, the excitation thresholds for the cochlear nerve are predicted to be quite uniform across electrode contact for normal bone density, conforming with the clinical observation where monopolar electrode coupling is used. The absolute value of excitation thresholds is also very much in line with the values encountered clinically. Although this flat profile is maintained with increasing bone conductivity for the full-band design (Fig. 4.3, left panels), the plate electrode design (right panels) is predicted to show more threshold increase for basal contacts than for apical contacts. This may indicate a reduction in efficiency for the plate contacts when more distant from their target neurons and when current leaks more easily through the scala tympani walls.

In Figure 4.2, there is a considerable drop in plate electrode cochlear nerve excitation threshold as the array is moved from a lateral to a medial location. Although this effect is also observed clinically, the model may overestimate it. This effect is much reduced for either the half-band or the full-band design, which shows little threshold change as a result of their move from the lateral to the medial position. The hypothesis explaining this would be that the field generated by the banded array results in a greater leakage of

current through the spiral ligament. There are few indications from the reported literature as to whether this difference is observed clinically.

Considering the influence of the position of the electrode array on FNS, Figure 4.2 shows that this phenomenon is more likely for electrode arrays in the lateral position than when positioned medially; this effect observed for all 3 electrodes modeled. At higher bone conductivities, this seems to be due to an increase in the cochlear nerve MCLs as a result of reduced current density in the scala tympani rather than to a decrease in the FN thresholds. For normal bone conductivity, the effect of an increased distance to the cochlear nerve in the case of laterally placed electrodes appears to be relatively small. These results also seem to match clinical reports.

In conclusion, the results obtained with the computational model have confirmed the clinical observation of increased FNS in cases of advanced cochlear otosclerosis with demineralization of the otic capsule. Rather than a decreased FN threshold, it is the increased levels of cochlear stimulation that is the main factor. On the basis of this finding, it is predicted that an electrode array with an increased bulk of carrier at the lateral side of the stimulating electrode contact would be less likely to produce FNS and hence might convey a clinical benefit.

References

Balkany, T.J., Eshraghi, A.A., Yang, N. 2002. Modiolar proximity of three perimodiolar cochlear implant electrodes. Acta Otolaryngol 122, 363-9.

Briaire, J.J., Frijns, J.H. 2000. Field patterns in a 3D tapered spiral model of the electrically stimulated cochlea. Hear Res 148, 18-30.

Briaire, J.J., Frijns, J.H. 2005. Unraveling the electrically evoked compound action potential. Hear Res 205, 143-56.

Frijns, J.H., Briaire, J.J., Grote, J.J. 2001. The importance of human cochlear anatomy for the results of modiolus-hugging multichannel cochlear implants. Otol Neurotol 22, 340-9.

Frijns, J.H., Kalkman, R.K., Vanpoucke, F.J., Bongers, J.S., Briaire, J.J. 2009. Simultaneous and non-simultaneous dual electrode stimulation in cochlear implants: evidence for two neural response modalities. Acta Otolaryngol 129, 433-9.

Frijns, J.H.M., Briaire, J.J., Schoonhoven, R. 2000. Integrated use of volume conduction and neural models to simulate the response to cochlear implants. Simulat Pract Theory 8, 75-97.

Hughes, M.L., Abbas, P.J. 2006. Electrophysiologic channel interaction, electrode pitch ranking, and behavioral threshold in straight versus perimodiolar cochlear implant electrode arrays. J Acoust Soc Am 119, 1538-47.

Jaekel, K., Aschendorff, A., Klenzner, T., Laszig, R. 2004. Results with the Contour cochlear implant in patients with cochlear otosclerosis. Laryngorhinootologie 83, 457-60.

Kelsall, D.C., Shallop, J.K., Brammeier, T.G., Prenger, E.C. 1997. Facial nerve stimulation after Nucleus 22-channel cochlear implantation. Am J Otol 18, 336-41.

Muckle, R.P., Levine, S.C. 1994. Facial nerve stimulation produced by cochlear implants in patients with cochlear otosclerosis. Am J Otol 15, 394-8.

Niparko, J.K., Oviatt, D.L., Coker, N.J., Sutton, L., Waltzman, S.B., Cohen, N.L. 1991. Facial nerve stimulation with cochlear implantation. VA Cooperative Study Group on Cochlear Implantation. Otolaryngol Head Neck Surg 104, 826-30.

Quaranta, N., Bartoli, R., Lopriore, A., Fernandez-Vega, S., Giagnotti, F., Quaranta, A. 2005. Cochlear implantation in otosclerosis. Otol Neurotol 26, 983-7.

Ramsden, R., Bance, M., Giles, E., Mawman, D. 1997. Cochlear implantation in otosclerosis: a unique positioning and programming problem. J Laryngol Otol 111, 262-5.

Ramsden, R., Rotteveel, L., Proops, D., Saeed, S., van Olphen, A., Mylanus, E. 2007. Cochlear implantation in otosclerotic deafness. Adv Otorhinolaryngol 65, 328-334.

Rotteveel, L.J., Proops, D.W., Ramsden, R.T., Saeed, S.R., van Olphen, A.F., Mylanus, E.A. 2004. Cochlear implantation in 53 patients with otosclerosis: demographics, computed tomographic scanning, surgery, and complications. Otol Neurotol 25, 943-52.

Sainz, M., García-Valdecasas, J., Garófano, M., Ballesteros, J.M. 2007. Otosclerosis: mid-term results of cochlear implantation. Audiol Neurootol 12, 401-6.

Schröder, J.M., Bohl, J., von Bardeleben, U. 1988. Changes of the ratio between myelin thickness and axon diameter in human developing sural, femoral, ulnar, facial, and trochlear nerves. Acta Neuropathol 76, 471-83.

Stakhovskaya, O., Sridhar, D., Bonham, B.H., Leake, P.A. 2007. Frequency map for the human cochlear spiral ganglion: implications for cochlear implants. J Assoc Res Otolaryngol 8, 220-33.

van der Beek, F.B., Boermans, P.P., Verbist, B.M., Briaire, J.J., Frijns, J.H. 2005. Clinical evaluation of the Clarion CII HiFocus 1 with and without positioner. Ear Hear 26, 577-92.

Vanpoucke, F.J., Zarowski, A.J., Peeters, S.A. 2004. Identification of the impedance model of an implanted cochlear prosthesis from intracochlear potential measurements. IEEE Trans Biomed Eng 51, 2174-83.

Verbist, B.M., Frijns, J.H., Geleijns, J., van Buchem, M.A. 2005. Multisection CT as a valuable tool in the postoperative assessment of cochlear implant patients. AJNR Am J Neuroradiol 26, 424-9.

Verbist, B.M., Joemai, R.M., Teeuwisse, W.M., Veldkamp, W.J., Geleijns, J., Frijns, J.H. 2008. Evaluation of 4 multisection CT systems in postoperative imaging of a cochlear implant: a human cadaver and phantom study. AJNR Am J Neuroradiol 29, 1382-8.

Youssef, O., Rosen, A., Chandrasekhar, S., Lee, H.J. 1998. Cochlear otosclerosis: the current understanding. Ann Otol Rhinol Laryngol 107, 1076-9.